

Supplementary Information

Resonator Embedded Photonic Crystal Surface Emitting Lasers

Zijun Bian^{1*}, Xingyu Zhao¹, Jingzhao Liu¹, Daehyun Kim^{1,2}, Adam F. McKenzie¹, Stephen Thoms¹, Paul Reynolds¹, Neil D. Gerrard¹, Aye S.M. Kyaw¹, James Grant¹, Katherine Rae¹, Jonathan R. Orchard³, Calum H. Hill³, Connor W. Munro^{1,3}, Pavlo Ivanov³, David T. D. Childs³, Richard J. E. Taylor³, and Richard A. Hogg^{1,2}

1. Photonic Crystal Band Structure

Figure S1(a) shows experimentally obtained band-structure from a 1.5 μm PCSEL structure, and results of simulation of the band-structure. The PCSEL structure and band-structure measurement are described in the manuscript. Simulation is made by plane-wave expansion utilising modal indices from a 1D solution of Maxwell's equations for the atom and field regions of the photonic crystal, and is also plotted. The inset shows an expanded version, to highlight the degenerate and non-degenerate bands.

Figure S1(b) shows the electric field distribution within the PCSEL. Black circles represent the edge of the atom and black arrows represent in-plane electric field with arrow size representing intensity. The in-plane magnetic fields which are periodic in either the vertical direction (mode A) or horizontal direction (mode B) while the electric field vectors arising from (mode C) and (mode D) are anti-symmetric about the centre of the atom. Hence, mode A and mode B would give leaky modes, while mode C and mode D would give non leaky modes^{S1}. High scattering normal to the surface is observed from the longer wavelength as leaky modes. The modes that make up the shorter wavelength are non-leaky and are candidates for the lasing mode due to their

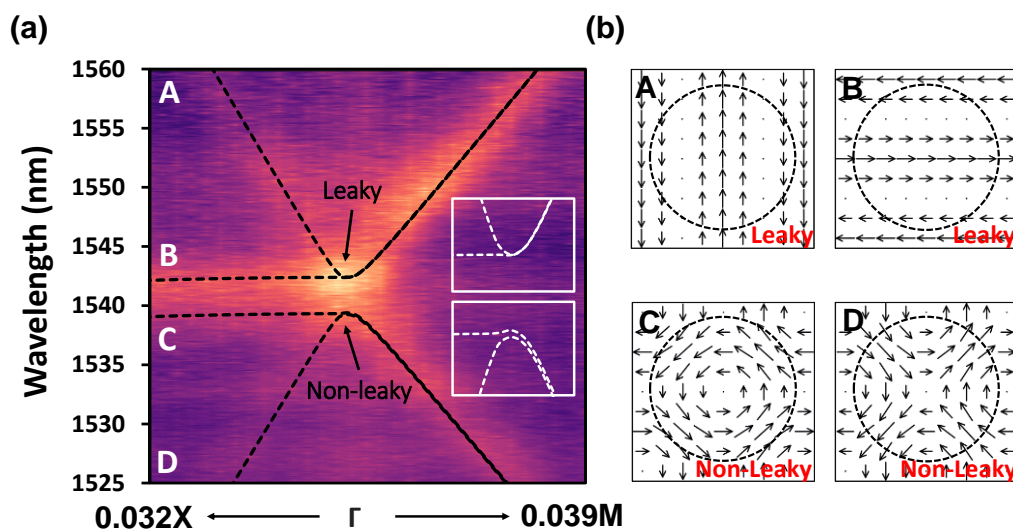


Fig. S1. (a)The PCSEL band structure measured well below I_{th} . The black dotted lines represent the modelled band structure. The inset shows the amplified degenerate and nondegenerate band edges. (b)The corresponding simulated electric fields for each mode.

low out-of-plane scattering and lower threshold gain. It is also noticed by tuning the hole radii in a square lattice PhC, the lowest threshold gain can exist alternately in both non-leaky modes (C&D)^{S2}. In this work, for a circular atom with radius of $0.4a$, the initial lasing mode can be found at mode D.

2. Effect of In-Plane 1D and 2D Coupling on the Resonator

In order to understand the effect of in-plane coupling on the propagation of light, and the existence of clearly defined path-lengths between resonator mirrors, we utilised our recently developed probabilistic Markov chain simulation^{S3}. This model considers the PCSEL as an array of matrix elements (each PhC atom) containing light propagating in the four in plane directions ($\pm x$, $\pm y$). Optical power is added, and scattering is calculated at each time step until convergence of the optical mode is obtained, allowing the effect of aspect ratio, boundary mirrors, coupling coefficients and PCSEL order (number of periods) on the in-plane optical loss and mode shape to be explored.

In this work, we utilise a similar approach to the aforementioned, injecting light from the boundary and determining the in-plane emission from the PCSEL as a function of time. Figure S2 shows a schematic of the model at $t=0$, where light is injected into matrix elements at the boundary as shown. This light is propagated within the modelled PCSEL structure, with scattering at each matrix element, corresponding to fractional power scattering, determined from experimentally determined values^{S4}. This scattering is repeated for each element at each time step. In this case, " $\kappa L \sim 2$ " corresponds to $L = 500$ periods with a period constant 400nm . The corresponding coupling coefficients κ_{1D} and κ_{2D} are 113.2cm^{-1} and 2.4cm^{-1} , respectively. As κ_{1D} is scaled, so κ_{2D} is scaled by the same amount. For example, " $\kappa L \sim 10$ " corresponds to $\kappa_{1D} = 113.2 \times 5\text{cm}^{-1}$ and $\kappa_{2D} = 2.4 \times 5\text{cm}^{-1}$. The values of utilized κ_{1D} and κ_{2D} are determined by simulation and analysis of the band structure for our $1.3\mu\text{m}$ devices^{S5}. The time-step is the time for light to travel from one matrix element (a PhC atom) to the next nearest neighbour.

Figure S3 plots the edge-emitted power as a function of time step for various κL . Two extreme cases can be seen. For $\kappa L = 0.5$, low levels of scattering out of the PCSEL are observed at all time steps, and this value gradually decays with time-step. A clear peak is observed at time step=500, corresponding to light traversing the length of the cavity with no scattering. With increasing κL , the optical power emitted at the edge at early times increases and the optical power emitted at $t=500$ reduces. For $\kappa L = 10$, no peak is observed at $t=500$. These results indicate that $\kappa L \ll 10$ is required to realise a REPCSEL. A value of $\kappa L \sim 2$ is adopted in the work here.

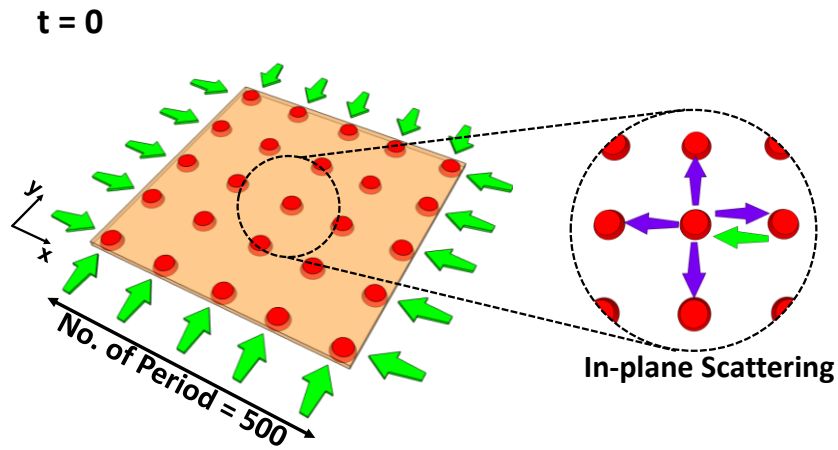


Fig. S2. Schematic of the probabilistic Markov chain simulation at $t=0$. The number of PhC periods is 500. Green arrows represent the incident light at the boundary. The insert shows possible scattering events at each PhC atom (purple arrows).

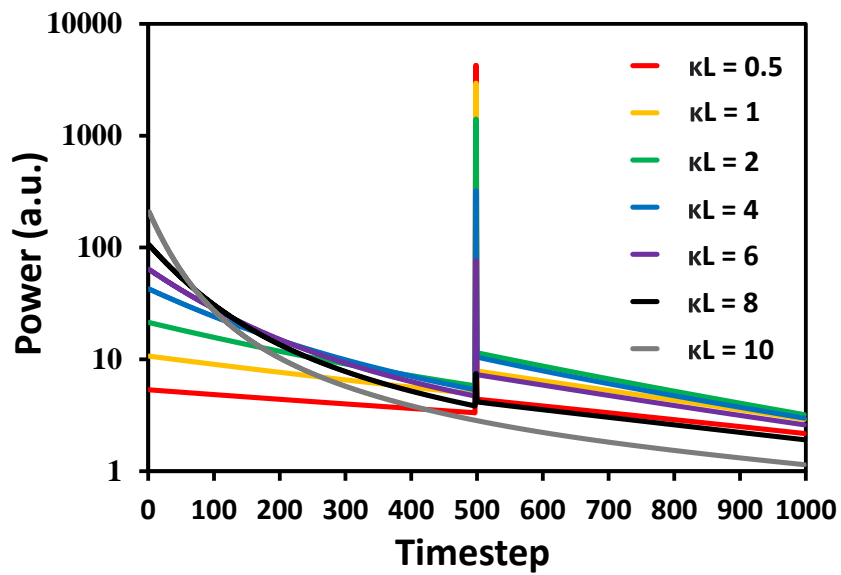


Fig. S3. Simulated in-plane power loss as a function of time for different values of κL according to the probabilistic Markov chain model in Fig. S2.

3. Band Structure of 1.3 μm REPCSEL as a Function of Current

Figure S4 plots the band-structure of 1.3 μm PCSELS as a function of drive current. Analysis of this data is presented in Fig. 4(d) of the manuscript.

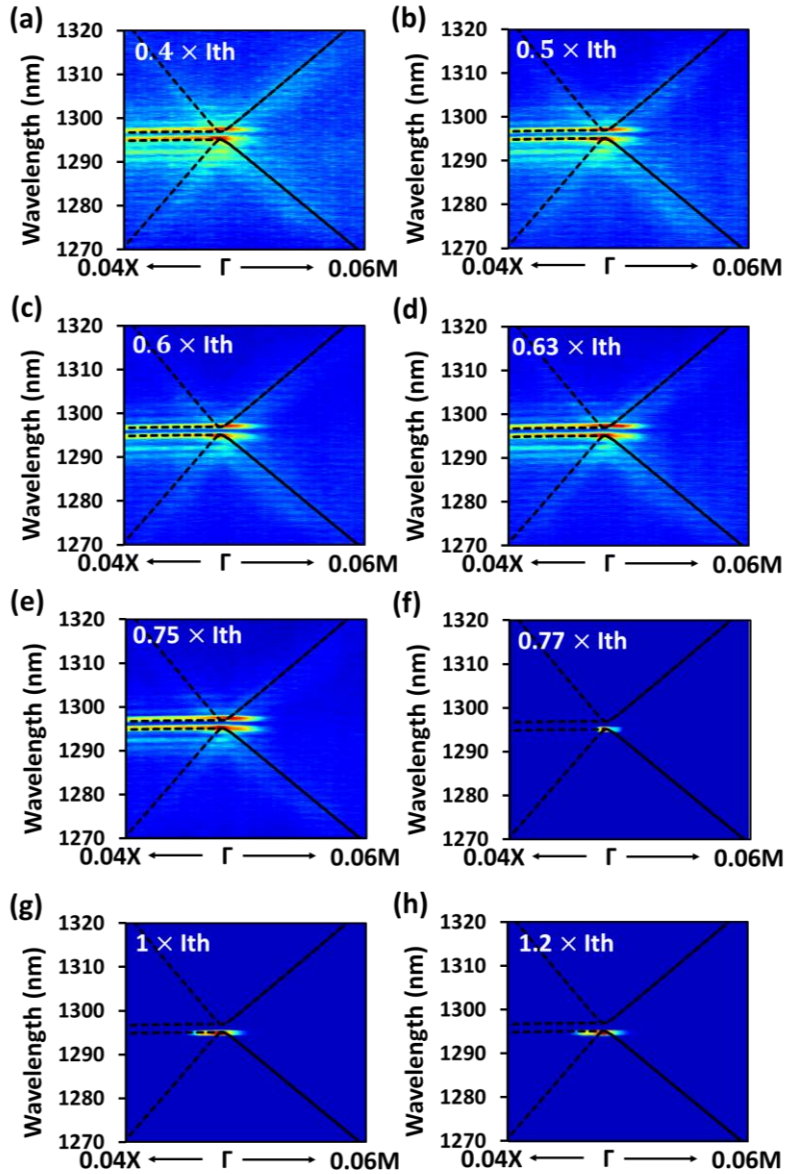


Fig. S4. Photonic band-structure of a 1.3 μm REPCSEL at (a) $0.4I_{\text{th}}$, (b) $0.5I_{\text{th}}$, (c) $0.6I_{\text{th}}$, (d) $0.63I_{\text{th}}$, (e) $0.75I_{\text{th}}$, (f) $0.77I_{\text{th}}$, (g) $1.0I_{\text{th}}$, (h) $1.2I_{\text{th}}$. Simulated PCSEL band-structure is shown schematically in (a).

4. Tuning the DBR target wavelength of the 1.5 μ m REPCSELs

Figure S5 explores the tuning of the alignment of the Fabry-Perot resonance effect and the photonic crystal band-structure, in this case for a 1.5 μ m structure. Here, we compare a PCSEL, and REPCSEL structures with different DBR structures targeting different wavelengths to tune the envelope of resonance peaks through the PhC band-structure (1550nm, 1542nm, 1534nm). In doing so, different resonance conditions can be applied to the modes at the Γ_2 point, selectively enhancing surface emission. Figure S5(a) shows the band-structure for a conventional PCSEL device (no DBR induced resonance). Overlaid is the calculated band-structure, and leaky (non-lasing) and non-leaky (possible lasing modes). Figure S5(b) schematically shows how different DBR target wavelengths vary with the band modes at Γ_2 point. It is noticed that although modes C&D are non-degenerated (as shown in Fig. S1), they are considered to be enhanced simultaneously by the same amount of IREF value due to a small mode splitting (<0.15 nm) from the low coupling. Figures S5(c-h) discuss the band-structure for the three REPCSELs in more detail. Figure S5(c) shows the band-structure for a device with a DBR targeting wavelength λ_1 (1550nm). It can be observed that the previously “silent” C&D, is now the strongest surface scattering Γ_2 point mode. Figure S5(d) shows the simulated overlap of the resonator IREF with the band-structure indicating a ~ 30 times increase in the scattering from C&D as compared to A&B. Figure S5(e) shows band-structure with similar intensities of the two modes (leaky & non-leaky) where the DBRs target 1542nm (λ_2). Here Fig. S5(f) shows a ~ 7 times higher IREF for the “non-leaky” bands C&D. Figure S5(g) shows a band structure more similar to the PCSEL case for a DBR targeting 1534nm (λ_3). In this case, IREF values for the A&B, and C&D are expected to be almost equivalent.

Figure S6 replots band-structure data from Fig. S5 of the manuscript. Here, a greyscale is used, with thresholds selected to highlight peaks in the spectra that make up the band-structure image. The effect of tuning the DBR target wavelength is highlighted. Three different DBR period constants with target wavelengths (a_1 : 1550nm; a_2 : 1542nm a_3 :1534nm). Plotted in red are the calculated IREF value from the simulated reflectivity curves for the boundary DBR structures, showing good agreement with experiment. A tuning of DBR target wavelength is obtained as expected when changing the DBR period.

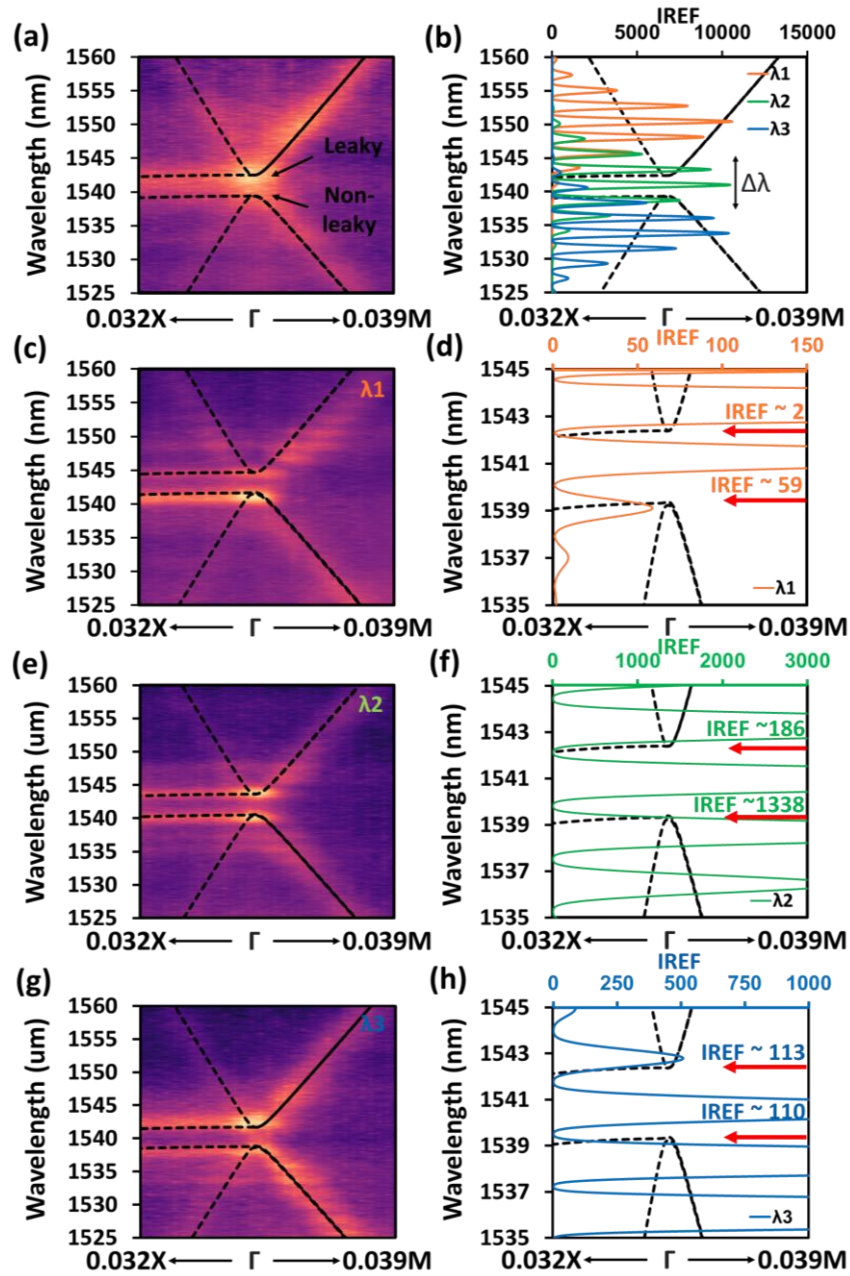


Fig. S5. (a) The measured band structure of a 1.5μm REPCSEL with simulated band structure (b). The calculated IREF of the REPCSEL with various target wavelengths ($\lambda_1 = 1550\text{nm}$, $\lambda_2 = 1542\text{nm}$, $\lambda_3 = 1534\text{nm}$). (c) (e) (g) The corresponding measured band structure of the REPCSEL with DBR target wavelengths $\lambda_1 = 1550\text{nm}$, $\lambda_2 = 1542\text{nm}$, $\lambda_3 = 1534\text{nm}$, respectively. (d) (f) (h) The calculated IREF results aligned with the simulated PhC band edge.

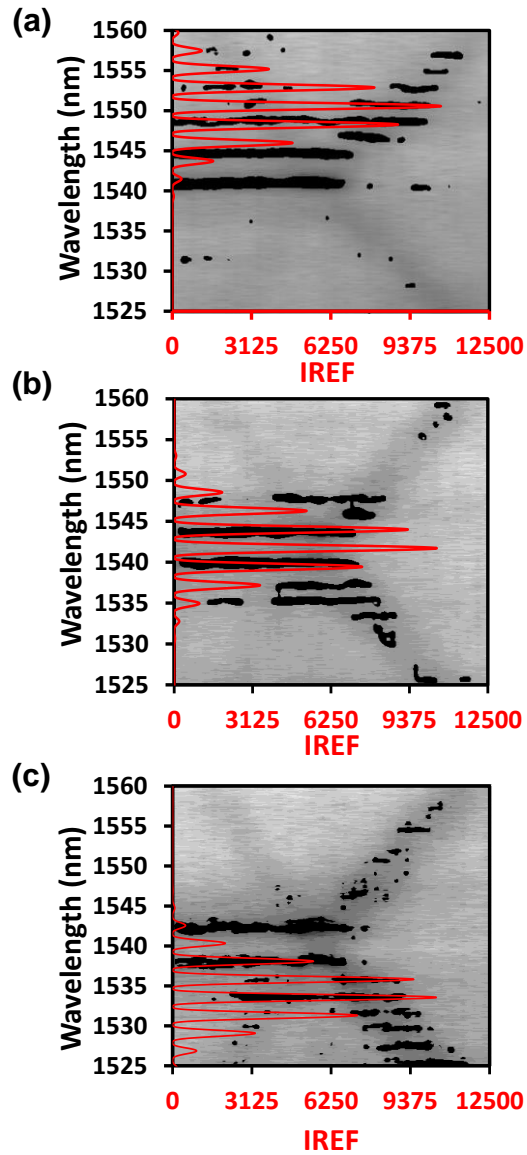


Fig. S6. Visualisation of band-structure of a 1.5 μm REPCSEL with DBR periods targeting (a) 1550nm (b) 1542nm (c) 1534nm. A greyscale is used, with thresholds selected to highlight peaks in the spectra that make up the band-structure image.

5. Band Structure Measurement Apparatus

Details are described in the methods section of the manuscript.

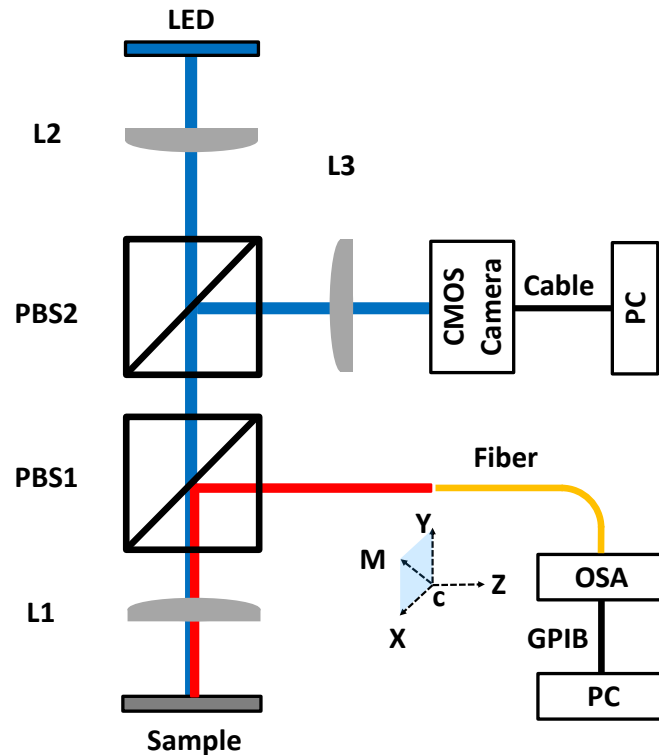


Fig. S7. Schematic of the measurement apparatus for band-structure analysis. L1 is a coated aspheric lens; L2 and L3 are plano-convex lenses. PBS1 & 2 are the pellicle beam splitters; OSA is an optical spectrum analyzer with a spectral resolution of 0.1nm.

References

- S1. Kurosaka, Y., Sakai, K., Miyai, E. & Noda, S. Controlling vertical optical confinement in two-dimensional surface-emitting photonic-crystal lasers by shape of air holes. *Opt. Express* **16**, 18485–18494 (2008).
- S2. Yokoyama, M. & Noda, S. Finite-difference time-domain simulation of two-dimensional photonic crystal surface-emitting laser. *Opt. Express* **13**, 2869 (2005).
- S3. Liu, J., Gao, Y., Ivanov, P., Harvey, P., Hogg, R., Probabilistic Markov chain modelling of photonic crystal surface emitting lasers, *App. Phys. Lett.* **123**, 261107 (2023).
- S4. Hirose, K. *et al.* Watt-class high-power, high-beam-quality photonic-crystal lasers. *Nat. Photonics* **8**, 406–411 (2014).
- S5. Sakai, K., Miyai, E. & Noda, S. Coupled-wave model for square-lattice two-dimensional photonic crystal with transverse-electric-like mode. *Appl. Phys. Lett.* **89**, 021101 (2006).